

## Research Article

# Comparison of Precipitated Calcium Carbonate/Poly(lactic Acid) and Halloysite/Poly(lactic Acid) Nanocomposites

Xuetao Shi,<sup>1,2</sup> Guangcheng Zhang,<sup>1</sup> Cristina Siligardi,<sup>3</sup> Guido Ori,<sup>3</sup> and Andrea Lazzeri<sup>2</sup>

<sup>1</sup>Department of Applied Chemistry, School of Science, Northwestern Polytechnical University, Xi'an 710072, China

<sup>2</sup>Department of Chemical Engineering, Industrial Chemistry and Materials Science, University of Pisa, Via Diotisalvi 2, 56126 Pisa, Italy

<sup>3</sup>Department of Chemistry, University of Modena and Reggio Emilia, 41100 Modena, Italy

Correspondence should be addressed to Xuetao Shi; [totalsxt@126.com](mailto:totalsxt@126.com) and Andrea Lazzeri; [a.lazzeri@ing.unipi.it](mailto:a.lazzeri@ing.unipi.it)

Received 13 August 2014; Revised 7 February 2015; Accepted 8 February 2015

Academic Editor: Xuping Sun

Copyright © 2015 Xuetao Shi et al. This is an open access article distributed under the Creative Commons Attribution License, which permits unrestricted use, distribution, and reproduction in any medium, provided the original work is properly cited.

PLA nanocomposites with stearate coated precipitated calcium carbonate (PCC) and halloysite natural nanotubes (HNT) were prepared by melt extrusion. The crystallization behavior, mechanical properties, thermal dynamical mechanical analysis (DMTA), and the morphology of the PCC/PLA, HNT/PLA, and HNT/PCC/PLA composites were discussed. Compared to halloysite nanotubes, PCC nanoparticles showed a better nucleating effect, which decreased both the glass transition and cold crystallization temperatures. The tensile performance of PLA composites showed that the addition of inorganic nanofillers increased Young's modulus but decreased tensile strength. More interestingly, PLA composites with PCC particles exhibited an effectively increased elongation at break with respect to pure PLA, while HNT/PLA showed a decreased ultimate deformation of composites. DMTA results indicated that PLA composites had a similar storage modulus at temperatures below the glass transition and the addition of nanofillers into PLA caused  $T_g$  to shift to lower temperatures by about 3°C. The morphological analysis of fractures surface of PLA nanocomposites showed good dispersion of nanofillers, formation of microvoids, and larger plastic deformation of the PLA matrix when the PCC particles were added, while a strong aggregation was noticed in composites with HNT nanofillers, which has been attributed to a nonoptimal surface coating.

## 1. Introduction

PLA polymer is a biodegradable thermoplastic derived from a renewable resource [1–3]. PLA polymer has received much attention not only as alternative to petrochemical plastics but also because of its high strength and stiffness, biocompatibility, and thermal processability. PLA is considered as a potential material in many fields such as biomedicine, packaging, and films [4]. However, its toughness, heat resistance, and gas barrier properties are not satisfactory and then its application for commercial products is limited because of those inherent weaknesses. The most extensively used methodology to improve PLA properties is to blend PLA with different plasticizers and (biodegradable or nonbiodegradable) polymers. Available plasticizers are glycerol, citrate ester, PEG, and PPG which are used to lower the glass transition temperature and increase ductility and processability [5, 6]. Meanwhile,

a lot of research work has been carried out on PLA polymer blended with other biodegradable polymers such as poly(3-hydroxybutyrate) (PHB) and poly( $\epsilon$ -caprolactone) (PCL) without compromising the biodegradability of PLA [7, 8]. Recently, PLA based nanocomposites are also investigated with nanoparticles, such as calcium carbonate, montmorillonite clay, and natural cellulose fibers [4, 9, 10]. In principle, rigid nanoparticles can substantially improve toughness more efficiently than rubber particles, when a good dispersion is achieved, since both stiffness and toughness can be balanced [11, 12]. The properties of this biodegradable PLA might be enhanced by the incorporation of nanoscale reinforcements as reported in the literature.

In this work, nanoprecipitated calcium carbonate (PCC) particles were added into the PLA as filler toughening agents. Calcium carbonate is the mostly widely used filler in polymers and enables increasing toughness without loss

TABLE I: Composition and crystallization properties of PLA composites.

Code	Composition				Isothermal crystallization			Thermal properties of PLA composites					
					$n$	$\log K$	$t_{1/2}$ (min)	$T_g$ ( $^{\circ}\text{C}$ )	$T_{cc}$ ( $^{\circ}\text{C}$ )	$\Delta H_{cc}$ (J/g)	$T_{m1}$ ( $^{\circ}\text{C}$ )	$T_{m2}$ ( $^{\circ}\text{C}$ )	$\Delta H_m$ (J/g)
PHC 1	PLA	HNT	PCC	100/0/0	2.298	-3.791	37.7	61.8	109.9	25.56	148.2	156.0	30.69
PHC 2	PLA	HNT	PCC	95/5/0	2.476	-3.831	31.2	62.1	103.8	25.62	146.9	155.0	27.94
PHC 3	PLA	HNT	PCC	90/0/10	2.234	-3.199	25.5	60.3	96.9	25.03	145.9	155.8	29.31
PHC 4	PLA	HNT	PCC	90/5/5	1.808	-2.184	<b>12.4</b>	57.9	98.4	27.41	146.8	156.7	30.68
PHC 5	PLA	HNT	PCC	85/5/10	2.656	-3.985	29.1	57.8	100.1	27.79	146.5	156.2	29.91
PHC 6	PLA	HNT	PCC	80/5/15	2.180	-3.357	20.3	58.9	99.0	25.65	145.7	156.2	30.83
PHC 7	PLA	HNT	PCC	75/5/20	2.339	-3.295	23.3	58.4	99.0	27.93	146.3	156.4	33.17
PHC 8	PLA	HNT	PCC	70/5/25	2.937	-4.062	21.9	58.7	97.6	19.34	145.6	155.5	32.91

The enthalpy of cold crystallization and melting is corrected according to the content of PLA in the composites.

in stiffness. In our former work [11], precipitated calcium carbonate nanoparticles coated with fatty acids were added into high-density polyethylene, and the impact strength of the polymeric composites was increased as the amount of stearic acid increased. We believed that the interfacial adhesion between PCC and HDPE was affected by the amount of fatty acid for the surface coating. A weaker interfacial interaction can achieve both a good dispersion of nanoparticles and debonding between fillers and the matrix during the fracture process, which are necessary factors for the improvement of toughness in polymer composites. The toughening mechanism for polymer nanocomposites with calcium carbonate has been well discussed for HDPE, PP, PVC, and ABS [13, 14]. However, little research work has been reported in the literature on PCC/PLA nanocomposites. In our study, this polymeric system was studied in relation to the thermal and mechanical properties, building upon our former experience on the application of calcium carbonate nanoparticles into polymers, with the purpose of improving the toughness of PLA.

Another type of nanofillers, a tubular clay material, halloysite nanotubes (HNTs), was also added to PLA, for the purpose of comparison. HNTs with molecular formula of  $\text{Al}_2\text{Si}_2\text{O}_5(\text{OH})_4 \cdot n\text{H}_2\text{O}$  are naturally occurring multiwalled inorganic nanotubes which have a similar geometry to carbon nanotubes (CNTs) [15, 16] but with a much lower cost. Xu and coworkers [17] carried out some research on polylactide-based composites with functionalized multiwalled carbon nanotubes (F-MWCNTs), which exhibited remarkable improvements in rheological properties in the molten state compared with pure PLA. Also F-MWCNTs acted as nucleating agent when applied to PLA. With similar structures and physical properties as CNTs, HNTs are receiving increasing attention in the field of polymeric composites based on the their following facts: HTNs possess high mechanical strength and modulus and a high aspect ratio, and they can easily be dispersed by shearing in the polymer matrix due to their relative low hydroxyl density compared to other layer silicates.

The aim of this study is to compare two different types of inorganic fillers on the final performance of PLA composites, such as the thermal behaviour and the mechanical properties,

especially fracture toughness. The nucleating effect of inorganic rigid nanoparticles on the crystallization behaviour of PLA composition was evaluated by the isothermal crystallization analysis. Meanwhile, the macromechanical properties and the microdeformation morphology of PLA composites were investigated.

## 2. Experimental

**2.1. Materials.** Semicrystalline extrusion grade PLA 2002 D (4% D-lactide, 96% L-lactide content, nominal average molecular weight  $M_w = 199590$ , and MFR 5–7 g/10 min) was purchased from Natureworks in pellet form. One of the filler particles was SOCAL precipitated calcium carbonate (PCC) obtained from Solvay Advanced Functional Minerals, Salin de Giraud, France. This type of PCC particles was surface treated with commercial stearin and the total organic content of the surfactant is about 13.5 wt%. The average particle size is about 70 nm and the specific surface area is about  $19 \text{ m}^2/\text{g}$ .

The other inorganic filler used was halloysite natural nanotubes supplied by Imerys Tableware Ltd. (Auckland, New Zealand). This type of halloysite nanotubes has a dimension with the diameter typically smaller than 100 nm and length typically ranging from about 500 nm to over  $1-2 \mu\text{m}$ .

**2.2. Sample Preparation.** The composites studied in this work were prepared by melt extrusion with the MiniLab II Haake Rheomex CTW 5 conical twin-screw extruder (Thermo Scientific Haake GmbH, Karlsruhe, Germany), at a screw rate of 90 rpm/min, a cycle time of 30 seconds, and with the extrusion barrel working at a temperature of  $190^{\circ}\text{C}$ . Prior to the extrusion, the PLA and fillers were dried at  $80^{\circ}\text{C}$  in a vacuum oven for eight hours. PCC/PLA composites were prepared with increasing fillers content from 5 wt% to 25 wt%. HNT/PLA composites were prepared with the nanotubes loading from 2 wt% to 10 wt%. Some compositions of PLA composites with both PCC and HNT are listed in Table I. After extrusion, the molten materials were transferred through a preheated cylinder to the Haake MiniJet II mini injection molder (Thermo Scientific Haake

GmbH, Karlsruhe, Germany), to obtain ASTM D638 V dog-bone tensile bars used for measurements and analysis. The molding parameters set were as follows: barrel: 180°C, mold: 50°C, injection pressure: 800 bar, and cycle time: 40 s. After molding, the specimens were placed in nylon bags with vacuum sealing to prevent moisture absorption.

### 2.3. Characterization

**2.3.1. Thermal Properties.** The crystallization behaviour of PLA composites was investigated by DSC technique with a TA Q200 instrument (TA Instruments, New castle, DE, USA) with nitrogen as purge gas. The DSC program was carried out firstly from 20°C to 190°C by a heating rate of 5°C/min. The sample was kept at 190°C for 5 minutes to remove the thermal history and then quenched to the isothermal temperature of 120°C, the crystallization temperature chosen in this work. The temperature was maintained at 120°C until complete crystallization of the sample. The Avrami equation was used for the kinetic crystallization study.

**2.3.2. Mechanical Properties.** Tensile tests were performed at room temperature, at a crosshead speed of 10 mm/min, by means of an Instron 4302 universal testing machine (Canton MA, USA) equipped with a 10 kN load cell and interfaced with a computer running the Testworks 4.0 software (MTS Systems Corporation, Eden Prairie MN, USA). At least five specimens for the tensile properties were tested according to the ASTM D 638.

**2.3.3. Dynamic Mechanical Properties.** Dynamic mechanical thermal analysis was carried out on pure PLA and PLA composites prepared with PCC or HNT fillers by means of a Gabo Eplexor 100 N (Gabo Qualimeter GmbH, Ahlden, Germany). Test bars were cut from the tensile bar specimens (size: 20 × 5 × 1.5 mm) and mounted in tensile geometry. The dynamic storage modulus and tan δ were recorded with a constant frequency of 1.00 Hz as a function of temperature from 0°C to 150°C with a heating rate of 2°C/min.

**2.3.4. Morphological Study.** The morphology of the composites was studied, by a scanning electron microscope (JEOL JSM-5600LV, Tokyo, Japan), by analyzing the fracture surfaces of samples, broken in liquid nitrogen. Prior to SEM analysis, all the surfaces were sputtered with a thin layer of gold.

## 3. Results and Discussion

**3.1. Crystallization Behavior of PLA Composites.** PLA crystallinity is a very important factor related to the mechanical and durability performance for molded applications. In this work, the isothermal crystallization of PLA composites was investigated at 120°C as the crystallization temperature from the molten state. The effect of the PCC particles and halloysite nanotubes on the PLA crystallization kinetics was compared by the crystallization half time by the isothermal tests. Figure 1 shows the DSC isothermal curves for pure PLA and

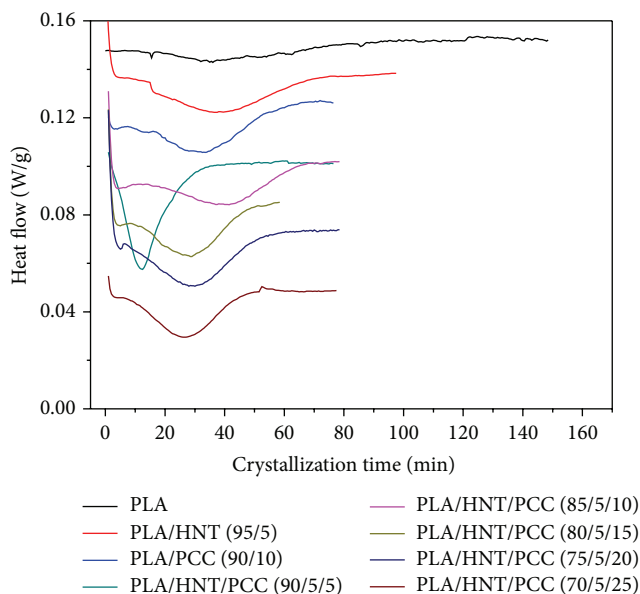


FIGURE 1: Selected isothermal DSC curves of PCC/PLA, HNT/PLA, and PCC/HNT/PLA ternary composites.

a selection of PLA composites. It is obvious that pure PLA has a very slow crystallization rate from the melt, which is a well-known result especially for the injection molded PLA products where PLA shows a low crystallinity or is almost amorphous. The degree of crystallinity and hence many important properties are largely controlled by the ratio of D to L enantiomers used, and to a less extent on the type of catalyst used [18]. The crystallization half time of pure PLA is about 37.7 min in this work. Our results are consistent with other works, which reported a half crystallization time in the range between 17 and 45 min, depending on the crystallization temperature, stereochemistry, and molecular weight [19]. Many works [20–22] discussed influence of the stereochemistry of PLA on the crystallization behaviour, since two optically active forms of lactic acid exist: L-lactic acid and D-lactic acid. Schmidt and Hillmyer [21] showed that the self-nucleation of PLA with stereocomplex (0.25–15 wt% PDLA into PLLA) was extremely effective compared to the traditional nucleating agents like talc. Self-nucleation is considered to be an ideal case for homopolymer crystallization due to an optimum dispersion of crystallites and the favourable interactions between the polymer melt and the polymer crystal fragments. In this work, only the effect of nanoparticles is investigated for the crystallization of PLA composites. PCC nanoparticles were applied as nucleating agents into polypropylene for the formation of  $\beta$  phase PP [23, 24]. Similar enhanced crystallization behaviour was also found when the HNT nanotubes were added into PP, which is attributed to the unique morphology with multiwalled inorganic tubes and rolled by some aluminosilicate layers [25]. Both the PCC and halloysite particles increase the crystallization rate from the melt and shorten the crystallization half time  $t_{1/2}$ , which is shown in the Table 1. Similar results were found in other researches for PLA/talc composites [19], in which it was

found that the addition of talc into the PLA can speed up the crystallization rate by over 65-fold over pure PLA for an isothermal temperature of 115°C. The most impressive increase in the crystallization rate has been found for the HNT/PCC/PLA composite with a composition of 05/05/90, which showed crystallization half time of only 12.4 min. As the content of PCC increases, the half crystallization time becomes longer again. This can be related to the possible formed percolation network with higher content of nanoparticle, which is also found in other PLA systems especially with high aspect ratio particles such as montmorillonite [2] and carbon nanotubes. The formed network is unfavorable for the PLA crystallization due to the prohibited chain mobility.

In this work, the results obtained from PLA nanocomposites during the DSC isothermal measurements, were analyzed by the Avrami equation:

$$1 - X(t) = \exp(-Kt^n), \quad (1)$$

where constant  $K$  is the crystallization rate,  $n$  is the Avrami exponent, and  $X(t)$  is the relative crystallinity at time  $t$ . The parameter  $K$  and  $n$  are related to the crystallization rate and to the type of nucleating and the geography of crystal growth. Figure 2 shows the plots of relative crystallinity of selected PLA composites against crystallization time. The crystallization half time is defined by the time where a relative crystallinity of 50% is reached. Pure PLA has the longest time to finish the crystallization from the melt. The Avrami plots of  $\log(-\ln(1 - X(t)))$  versus  $\log(t)$  are shown in Figure 3, where the intercept and slope of the best fitting lines are calculated as the value of  $\log K$  and  $n$ , respectively. The Avrami exponent  $n$  of both pure PLA and PLA composites is just below 3. In other words, this value means that the crystal growth occurred in 3 dimensions. In general, the nucleation stage and the crystal growth are more complicated for the polymeric composites due to the possibility that fillers can act as nucleating agents to increase the crystallization or to limit the normal crystal growth in some certain areas such as the interphase between fillers and polymer matrix [26], depending upon the interfacial adhesion.

In the literature, it is generally accepted that slowly crystallizing polymers tend to form a multilayer structure with an amorphous skin, a semicrystalline intermediate layer, and an amorphous core in their injection molded specimens [2], which is due to the thermal and stress crystallization during the injection process. However, crystallization of PLA from melt usually occurs in the temperature range from 80°C to 120°C [27]. The crystallization properties of PLA molded samples showed no structural gradient in PLA nanocomposites [27], which was explained by the combined effect of material crystallization ability and the injection molding conditions (50°C). In our work, the neat PLA exhibited no crystallization peak during cooling from melt state with a cooling speed of 20°C/min and this is consistent with the literature that no crystals form during cooling at this speed. For the pure PLA, therefore, the DSC sample for the isothermal tests was taken from the injected molded specimens, which is already quenched from the melting state by a fast cooling speed in 15 seconds to 50°C as the molding

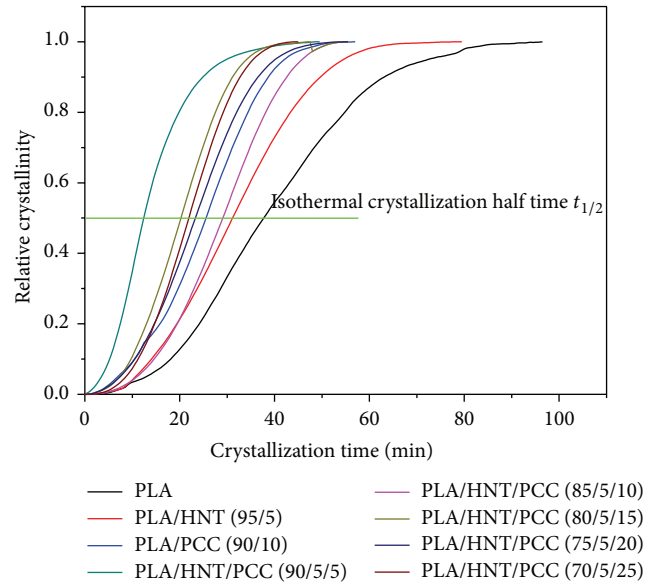


FIGURE 2: Plot of the relative crystallinity versus time from the isothermal crystallization.

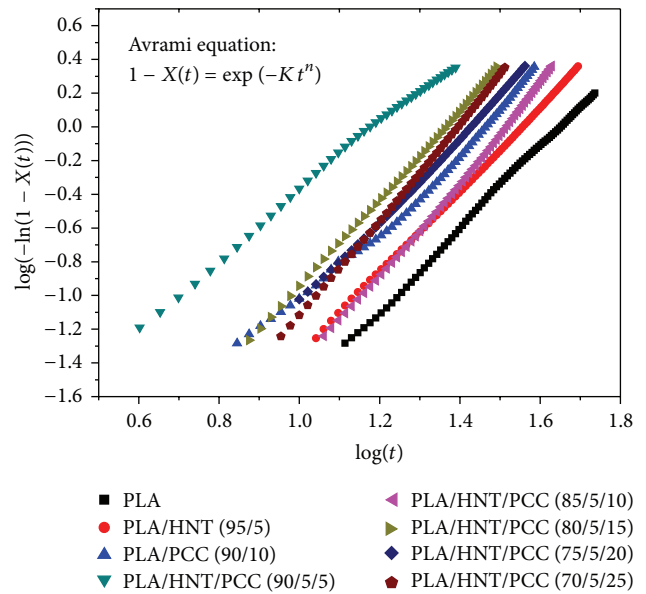


FIGURE 3: Linear Avrami plots of  $\log(-\ln(1 - X(t)))$  versus  $\log(t)$  of the selected PLA composites.

temperature. The characteristic thermal properties, such as glass transition temperature ( $T_g$ ), cold crystallization temperature ( $T_{cc}$ ), enthalpy of cold crystallization ( $\Delta H_{cc}$ ), melting temperature (two peaks  $T_{m1}$  and  $T_{m2}$ ), and enthalpy of fusion ( $\Delta H_m$ ), are marked in Figure 4 and those values are shown in Table 1. The addition of both PCC particles and halloysites nanotubes into PLA decreases the  $T_g$  by about 3°C. More impressively, the cold crystallization temperature (109.9°C) of pure PLA was decreased by the incorporation of PCC and HNT fillers, which also indicated the improved crystallization behaviour of PLA matrix with the presence

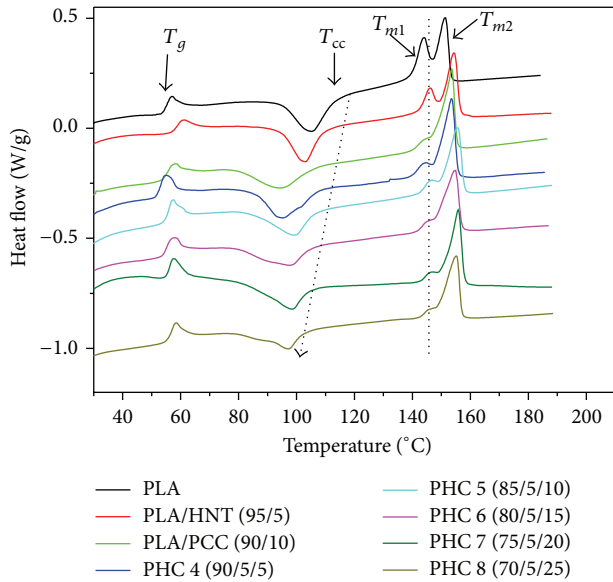


FIGURE 4: DSC traces of PLA molded composites with a heating speed of 5°C/min after quenching at 50°C.

of nanoparticles. The decreased glass transition temperature indicates the enhanced chain mobility of PLA polymer with the addition of particles attributed to the surface treatment of particles. Furthermore, the decreased cold crystallization temperature reveals that decreased crystallization induction period due to the presence of the already existing crystalline nuclei formed during injection process and the nanoparticles as heterogeneous nucleating agents. This result confirms the Avrami isothermal study that rigid inorganic particles like PCC can behave like nucleating agents in the PLA polymer. Meanwhile, the enthalpy of cold crystallization was slightly increased by the addition of nanoparticles compared to that of the pure PLA. This enhanced crystallization behaviour can be explained by the high surface area supplied by the nanoparticles and thus by the increasing number of nucleating sites for PLA matrix. The crystallinity of PLA nanocomposites can be determined from the difference between the enthalpy of fusion and that of cold crystallization, which is quite small compared to the theoretical melting enthalpy (93 J/g) [28], which means that the injection moulded PLA composites are almost in amorphous structure. There is not too much difference of the PCC composition on the crystallization behavior and all nanocomposites can increase the crystallizing speed of PLA in isothermal tests.

Another interesting point is that two melting peaks show in the DSC curves for pure PLA in Figure 4. For the nanocomposites with the PCC and HNT fillers, there is a progressive shift of lower temperature peak to the higher temperature. The two melting peaks are classic for the PLA thermal behavior due to reorganization of less perfect crystals, which have the same structure of the more perfect crystal but with a smaller lamella thickness [29]. Figure 4 clearly shows the shift of the first melting peak to higher temperatures in the PLA nanocomposites. We believe that

the improved crystallization rate favors the nucleation of larger amounts of already existing less perfect crystals with respect to the pure PLA polymer, resulting in the shift of melting temperature to higher part. Here PCC nanoparticles have a much more impressive influence on the reorganization of the PLA crystals.

There are slight differences of the half crystallization time of the HNT/PLA and PCC/PLA nanocomposites. More work will be carried out to discuss the influence of the PCC loading and the possibility of molded temperature on the crystallization behavior of PLA composites with the consideration of the mechanical properties and the morphology structures of the PLA composites.

**3.2. Mechanical Properties.** Pure PLA is well known with its high strength and stiffness. The strain-stress curves of PLA composites with PCC, halloysite, or both of those two types of nanoparticles are shown in Figure 5. The pure PLA shows the highest tensile strength but with a very small elongation at break of about 3.5%. The specimens of pure PLA fractured without any whitening or necking. The addition of both halloysite nanotubes and PCC particles into PLA decreases the tensile strength as shown in Figure 5. Furthermore, HNTs are more effective for the strength of PLA nanocomposites compared with PCC. More interesting, the addition of PCC can increase the elongation at break from about 3.5% for the pure PLA to about 10% of the PLA filled with 10 wt% of PCC particles as shown in Figure 5(b). Meanwhile, all the specimens of composites with PCCs show extensive stress whitening band over the whole gauge length. However, the elongation at break first increases to reach a maximum of about 12% as the maximum value when the PCC particles increase to be 15 wt% and then decreased with the further addition of PCC particles. However, the addition of the HNT nanotubes has little effect on the elongation at break of nanocomposites. From Figure 5(c), it is impressive of the little increased elastic modulus of HNT/PLA composites with respect to that of pure PLA. This result confirms that the HNT nanotubes are effective in the improvement of stiffness. The HNT/PCC/PLA ternary composites in Figure 5(a) show unstable mechanical properties as the increasing of PCC content in the composites except the relative increasing of elongation at break. Similar to the PLA/PCC system, the elongation at break of HNT/PCC/PLA composites first increases and then decreases with rising level of loading of PCC fillers, while the yield stress keeps decreasing when the fillers content increases. From the stress-strain curves of three different PLA composites, the effect of PCC coated with stearic acid on both the yield stress and the elongation at break can be explained by a decreased interfacial adhesion between PCC fillers and the PLA matrix in the presence of stearic acid in the interphase.

Young's modulus and the tensile stress of those three types of PLA nanocomposites are compared in Figures 6 and 7 as a function of the contents of nanoparticles in the PLA matrix. The tensile strength tends to decrease gradually as the fillers content increases in all the three PLA composites. The addition of 20 wt% of PCC decreased the tensile strength by 27%. Considering that the elongation at break of PCC/PLA

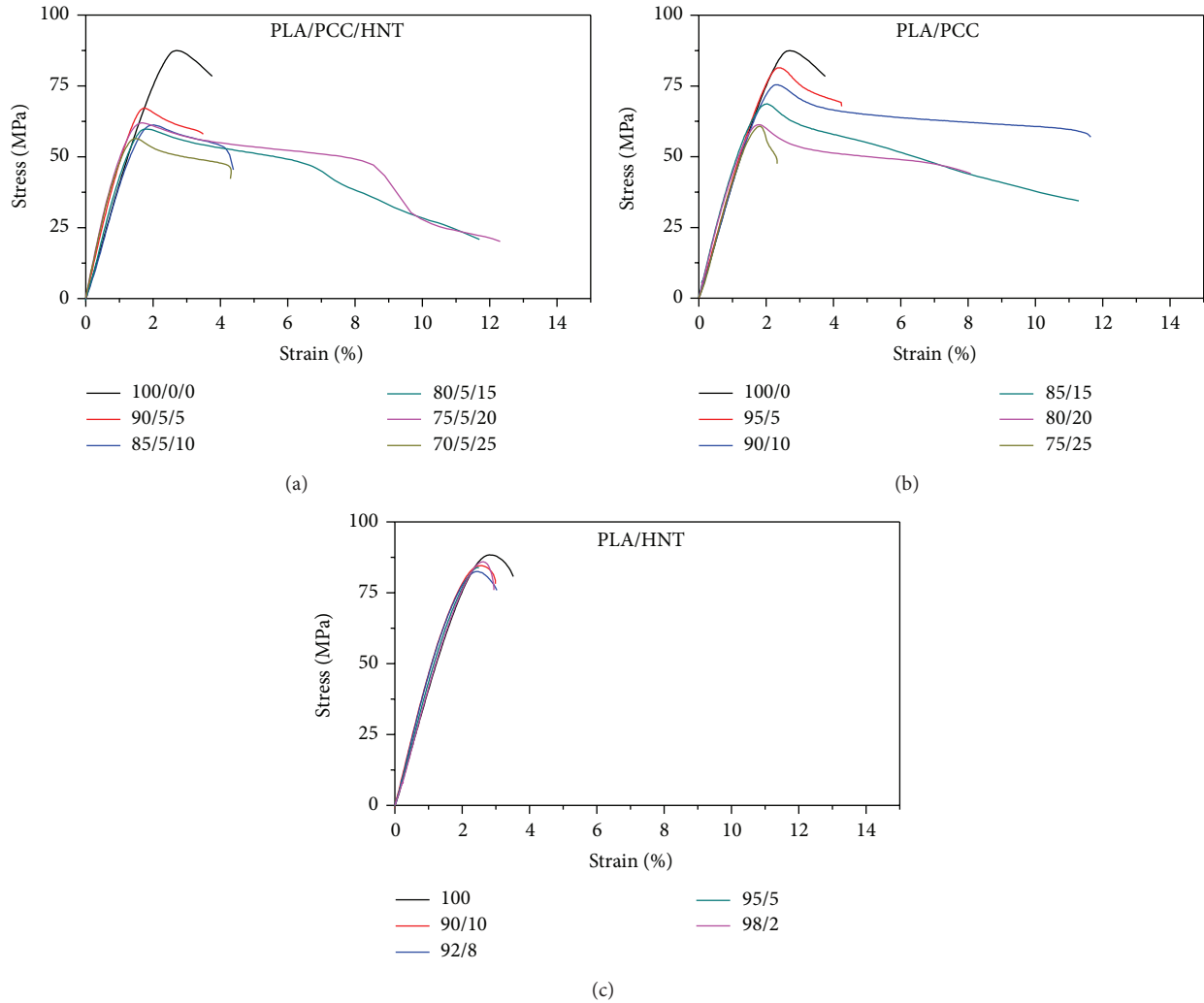


FIGURE 5: Strain-stress curves of (a) HNT/PCC/PLA ternary, (b) PCC/PLA, and (c) HNT/PLA composites.

composites is bigger than that of pure PLA, the decreased tensile stress is a reflection of both weaker interface adhesion between the nanoparticle and the polymer matrix and a plasticizing effect of surface coating. In our former work [11] for the HDPE toughened by PCC nanoparticles coated with stearic acid, similar weaker interface interaction between polyethylene and calcium carbonate particles allowed the improvement of the toughness of final nanocomposites. Here we believe that the surface modified PCC particles have a suitable interface interaction with PLA and this is responsible for the decreasing yield stress shown in the Figure 6. The weaker interfacial adhesion between rigid nanoparticles and the polymer is also reported to achieve debonding of nanoparticles from the matrix and then the improved toughness [29, 30].

The effect of HNT nanotubes in the PLA polymer shows higher Young's modulus with respect to the addition of PCC to PLA, which is due to the higher aspect ratio of HNT nanofillers. All those tensile results indicated that the HNT nanotubes and PCC particles have different effects on

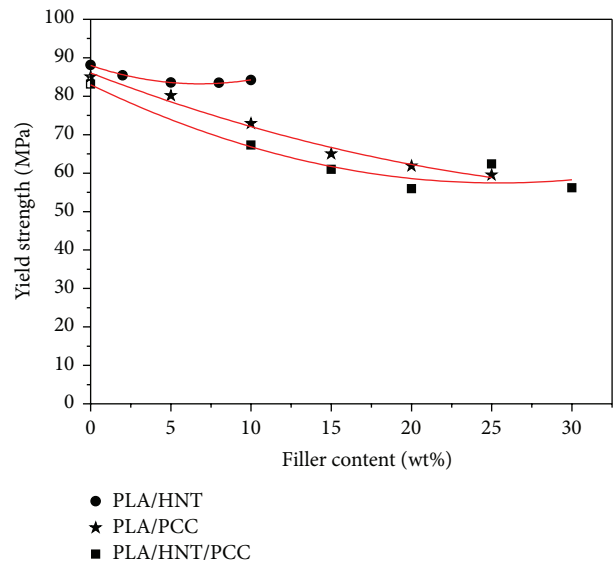


FIGURE 6: Tensile strength of PLA composites versus fillers content.

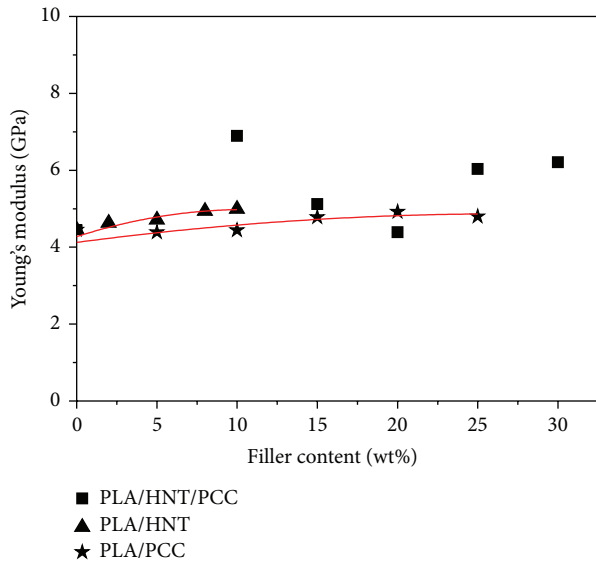


FIGURE 7: Young's modulus of PLA composites versus fillers content.

the toughness and stiffness on the PLA polymer. However, the HNT/PCC/PLA composites show the lowest yield stress and unstable Young's modulus when compared to the single filler systems. The lower tensile strength can be related to the lower particles/polymer interfacial adhesion or to the presence of flaws due to the aggregation of the fillers. Further morphology analysis will be able to justify the resulting decreasing of yield stress.

Figure 8 shows the dynamic storage modulus  $E'$  of pure PLA and PLA composites with PCC or HNT over a temperature range from 0°C to 150°C. Generally, the storage modulus of both pure PLA and PLA composites keeps stable over the temperature from 0°C to about 55°C. A lower storage modulus of PLA/PCC (95/5) composites can be explained by the lower interfacial adhesion due to the surface treatment of PCC, which is consistent with the mechanical tensile results. Then the storage modulus drops rapidly due to the glass transition. However, after this temperature range, the storage modulus increases rapidly with temperature, which is attributed to the well-known cold crystallization. However in the case of PCC and HNT, the storage modulus is not stable and shows a much lower value with respect to that of PLA in the cold crystallization region. There are two possibilities to explain the low storage modulus in PLA nanocomposites; one can be the enhanced mobility of PLA polymer chain and the other one is the smaller numbers of PLA molecular chains involved. At room temperature, the storage modulus shows not much difference between the neat PLA and PLA composites except the PLA composites with 5 wt% PCC. In others' research work [31, 32], the addition of inorganic particle shows a huge increase of the storage modulus below the glass transition temperature. Again this result matches with the decreased tensile strength with the addition of PCC particles due to the weaker interfacial adhesion between fillers and the matrix.

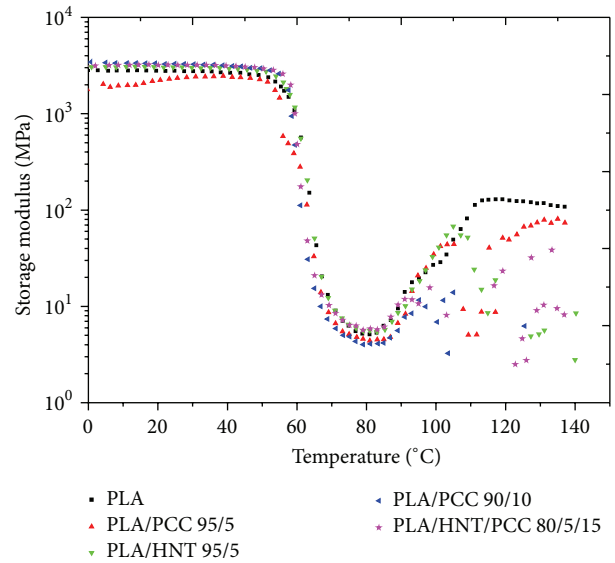


FIGURE 8: Temperature dependence of storage modulus  $E'$  of selected PLA composites.

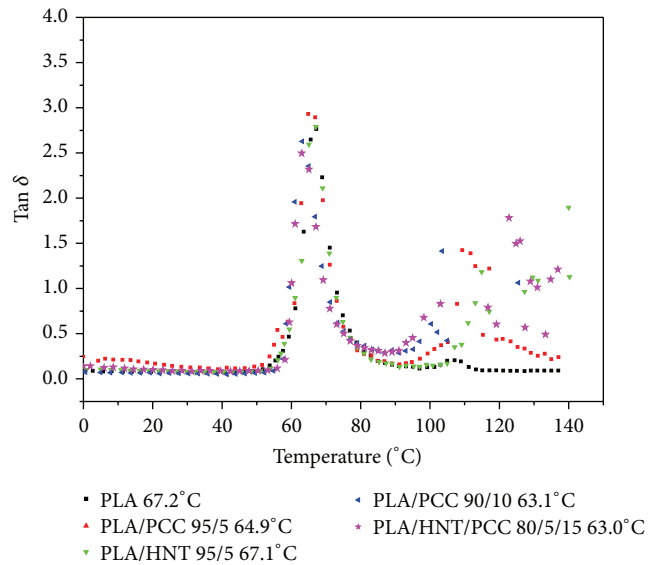


FIGURE 9: Temperature dependence of  $\tan \delta$  of the selected PLA composites.

In Figure 9, the  $\tan \delta$  curves of pure PLA, PLA composites with PCC or HNT or both of them are plotted against temperature. The pure PLA shows a glass transition temperature  $T_g$  at about 67.1°C according to the peak value of the  $\tan \delta$  curve. For the PLA composites, the  $T_g$  values decreased to about 63.0°C for PCC/PLA composites. The slight decrease of  $T_g$  is consistent with what is observed in tensile tests when the stearic acid coated PCC caused both a good dispersion of particles and weak interfacial adhesion with the PLA matrix. However, the addition of HNT nanotubes into PLA also showed a slight decrease of the  $T_g$  temperature, which contradicts with other reports according to which the glass

transition temperature tends to increase due to the addition of inorganic fillers. In other words, the addition of fillers into PLA polymer induced increased polymer chain mobility in the interphase zone. As it is well known, the glass transition is a complex phenomenon related to many factors such as the chain flexibility, molecular weight, branching, crosslinking, and intermolecular interaction. Papageorgiou and coworkers [31] discussed the thermal properties of PLA composites with multiwalled carbon nanotubes, montmorillonite, and silica nanoparticles. They reported impressive enhancement in the storage modulus for all three types of composites and a small increase of  $T_g$  (1–2°C), which was attributed to the physical crosslink caused by the interaction between fillers and PLA. Similar results were recorded for PLA composites with other nanoparticles such as clay [9], bentonite [31], microcrystalline cellulose [32], and natural fibers [10]. However a lower  $T_g$  transition temperature was reported for PLA modified with plasticizer, such as PPG [33], PEG [34], and glyceryl triacetate [35]. Similar shift in  $T_g$  shown for PCC/PLA composites with the PLA modified with plasticizers is consistent with the conclusion of Molnar et al. [36] that the stearic acid on the PCC surface acts as plasticizer.

About the cold crystallization occurring in the temperature range from about 80°C to 120°C, the pure PLA showed a very small peak in this range while the PLA composites give a much higher intensity peak also due to the cold crystallization of PLA matrix. In other words, more PLA chains are involved in the crystallization around the soft interphase zone. Meanwhile, there is a big improvement in the spherulites due to the presence of the inorganic fillers separated in the PLA matrix. Again, the effect of PCC as nucleating agents can be confirmed by  $\tan \delta$  curves.

**3.3. Morphology of PLA Nanocomposites.** The fracture surface of the tensile samples was investigated by the SEM technique as shown in Figures 10(a) to 10(d). The dispersion or distribution of nanofillers into the polymer matrix is an important topic for the high performance of polymeric nanocomposites in particular for the mechanical and thermal properties. Pure PLA, HNT/PLA, PCC/PLA, and HNT/PCC/PLA composites are compared in Figure 10. The surface of pure PLA is smooth without plastic deformation and a few fibrils were formed, typical of a fracture process dominated by crazing. Figure 10(b1) shows the fracture surface of PLA with only halloysite natural tubes at different magnifications. The whole surface in Figure 10(b2) shows the presence of big aggregation of halloysite natural nanotubes and this will cause early fracture, which is the explanation of the decreased yield strength in the tensile tests. However, a part of the PLA/HNT surface consists of uniform separated nanotubes, as shown in Figure 10(b3), some of which are pulled out with some holes left on the surface. This shows the potential of the application of HNT nanotubes taking advantage of their high surface area and their unique structure, in the case homogeneous dispersion could be reached. This will be left to some future work to try to carry out a surface coating for the natural nanotubes to decrease their aggregation and meanwhile to increase their compatibility between those hydrophilic fillers and the relatively hydrophobic polymer. The tensile

specimens of PLA/PCC nanocomposites, which exhibited the stress whitening during the tensile test, show a homogeneous fracture surface with the well separated PCC particles in Figure 10(c1) compared to the HNT nanotubes. The PLA matrix in the PLA/PCC composites has enhanced plastic deformation (in Figure 10(c2)) compared to that of pure PLA. This better dispersion of PCC particles is achieved by the surface coating with stearic acid, which effectively decreased the surface free energy of the calcium carbonate nanoparticles as reported in our former work [37]. Meanwhile, the interfacial adhesion between the PCC particles and PLA polymer is also influenced by the surface coating since debonding of calcium carbonate particles from the PLA matrix occurred during the tensile test and evidence of cavitations is shown in the Figure 10(c2). In other words, this debonding due to the weaker interfacial adhesion between PCC and PLA is responsible for the decreasing tensile strength and the increasing elongation at break for PLA composites when PCC particles are added and also is one of the most critical factors for the toughness improvement of PLA nanocomposites.

The addition of both PCC and HNT nanofillers into PLA does not change the aggregation of HNT and then the fracture surface showed different zones in Figure 10(d1). Figure 10(d2) shows a typical aggregate of HNTs and this zone represents a material flaw and will induce a decrease of mechanical properties. Another zone is shown in Figure 10(d2) where PCC particles are clearly visible as well as many microvoids due to the debonding of PCC particles from the PLA polymer. There is also the combination of the fibrillation of the PLA around the nanoparticles and the microvoids, which plays an important role in enhancing the toughness of the materials [38, 39]. Considering the mechanical properties in the tensile part, we believe that PCC nanoparticles are also potential nanofillers for the toughness improvement of PLA polymer.

## 4. Conclusion

PLA composites with PCC (coated with stearic acid) and HNT nanotubes were compared in this study. Isothermal crystallization study indicated both two nanofillers acted as nucleating agent by decreasing the half crystallization time and increasing the crystal growth rate. Additionally, the glass transition temperature was decreased by about 3°C when the PCC particles were added into PLA due to the enhanced mobility of PLA polymer chains. Similar  $T_g$  decrease resulted from the DMTA tests, which indicated a shift of  $\tan \delta$  peak (corresponding to  $T_g$ ), to the lower temperatures in the PLA composites. The tensile tests of PLA composites with PCC, HNT, or both of them showed different effects on the mechanical performance such as the yield stress, Young's modulus, and the elongation at break. The most impressive increase of ultimate deformation of PLA composites occurred when PCC fillers were present and the maximum elongation at break reached about 15%. However, the addition of HNT nanotubes resulted in decreased elongation at break of the PLA composites. Such mechanical difference is attributed to the nanoparticles dispersion in the matrix as the PCC was surface coated with stearate for achieving a uniform distribution and the HNTs were not coated and then possess



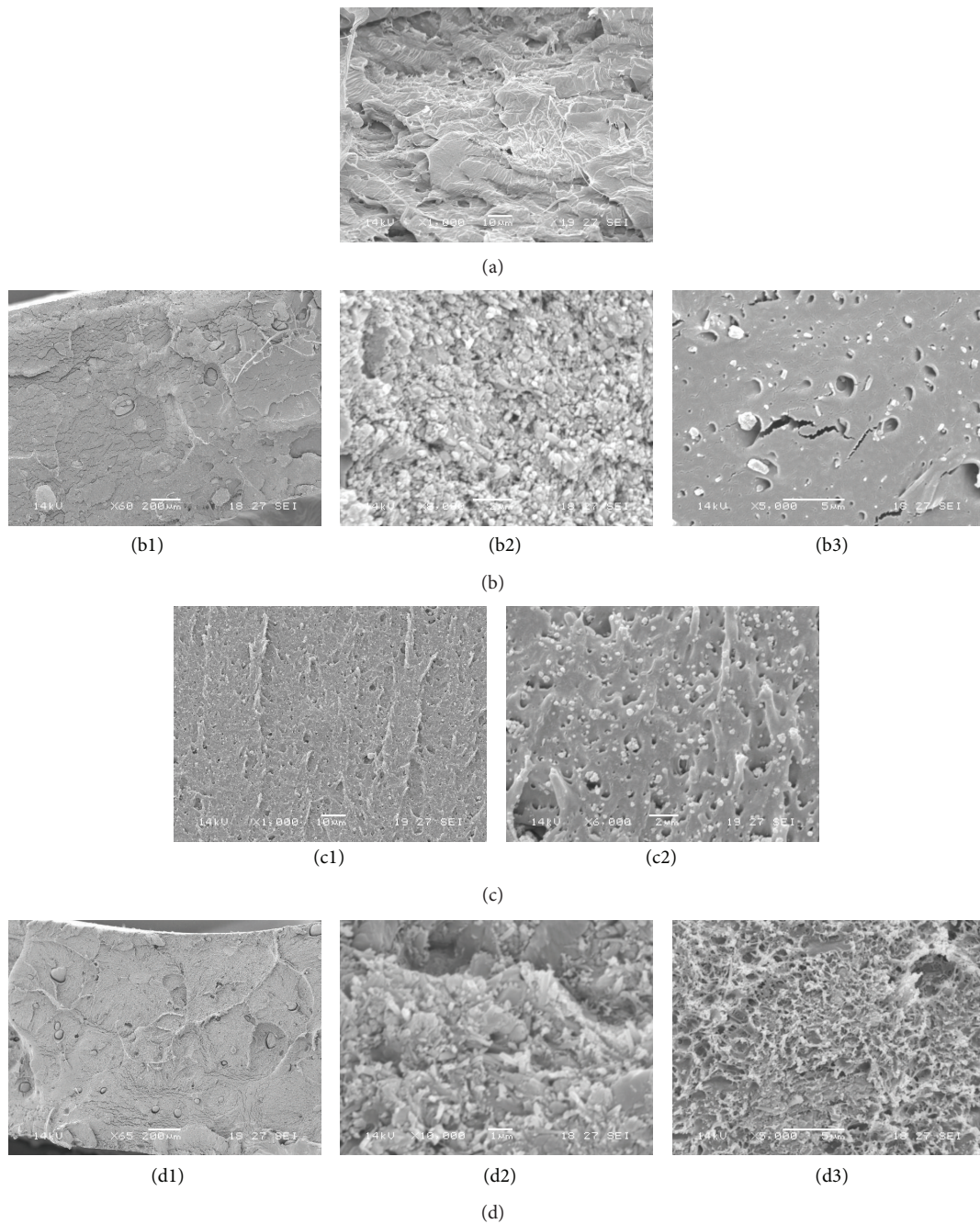


FIGURE 10: SEM micrographs of the fracture surface of tensile specimens: (a) pure PLA, (b) HNT/PLA (95/5) composites, (c) PCC/PLA (90/10) composites, and (d) HNT/PCC/PLA (80/5/15) ternary composites.

a much higher surface energy leading to the aggregation. These considerations were confirmed by the SEM morphological analysis. A weaker interfacial adhesion is proposed for the PCC surface coating with stearate, which is necessary for the microvoid formation and higher plastic deformation of the polymer matrix during the fracture process of PLA composites. Therefore, a good dispersion and easy debonding of the PCC particles together with the fibrillation of PLA matrix indicated the potential possibility of PCC for the toughness improvement of PLA composites.

### Conflict of Interests

The authors declare that there is no conflict of interests regarding the publication of this paper.

### Acknowledgments

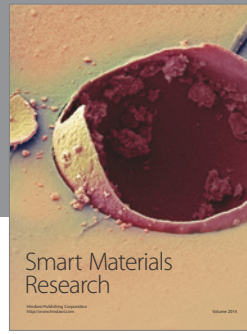
The authors wish to acknowledge the support from FP7 KBBE Project no. 212239 Forbioplast (Forest Resource Sustainability through Bio-Based Composite Development) and

also the support from National Natural Science Foundation of China (Grant no. 51303149) and the Fundamental Research Funds for the Central Universities (Grant no. 3102014JC01095).

## References

- [1] L. Jiang, B. Liu, and J. Zhang, "Properties of poly(lactic acid)/poly(butylene adipate-co-terephthalate)/nanoparticle ternary composites," *Industrial & Engineering Chemistry Research*, vol. 48, no. 16, pp. 7594–7602, 2009.
- [2] L. Jiang, J. Zhang, and M. P. Wolcott, "Comparison of polylactide/nano-sized calcium carbonate and polylactide/montmorillonite composites: reinforcing effects and toughening mechanisms," *Polymer*, vol. 48, no. 26, pp. 7632–7644, 2007.
- [3] A. Gandini, "Polymers from renewable resources: a challenge for the future of macromolecular materials," *Macromolecules*, vol. 41, no. 24, pp. 9491–9504, 2008.
- [4] R. M. Rasal, A. V. Janorkar, and D. E. Hirt, "Poly(lactic acid) modifications," *Progress in Polymer Science*, vol. 35, no. 3, pp. 338–356, 2010.
- [5] O. Martin and L. Avérous, "Poly(lactic acid): plasticization and properties of biodegradable multiphase systems," *Polymer*, vol. 42, no. 14, pp. 6209–6219, 2001.
- [6] E. Piorkowska, Z. Kulinski, A. Galeski, and R. Masirek, "Plasticization of semicrystalline poly(l-lactide) with poly(propylene glycol)," *Polymer*, vol. 47, no. 20, pp. 7178–7188, 2006.
- [7] Y. Takagi, R. Yasuda, M. Yamaoka, and T. Yamane, "Morphologies and mechanical properties of polylactide blends with medium chain length poly(3-hydroxyalkanoate) and chemically modified poly(3-hydroxyalkanoate)," *Journal of Applied Polymer Science*, vol. 93, no. 5, pp. 2363–2369, 2004.
- [8] M. E. Broz, D. L. VanderHart, and N. R. Washburn, "Structure and mechanical properties of poly(D,L-lactic acid)/poly( $\epsilon$ -caprolactone) blends," *Biomaterials*, vol. 24, no. 23, pp. 4181–4190, 2003.
- [9] M. Pluta, J. K. Jeszka, and G. Boiteux, "Polylactide/montmorillonite nanocomposites: structure, dielectric, viscoelastic and thermal properties," *European Polymer Journal*, vol. 43, no. 7, pp. 2819–2835, 2007.
- [10] K. Oksman, M. Skrifvars, and J.-F. Selin, "Natural fibres as reinforcement in polylactic acid (PLA) composites," *Composites Science and Technology*, vol. 63, no. 9, pp. 1317–1324, 2003.
- [11] A. Lazzeri, S. M. Zabarjad, M. Pracella, K. Cavalier, and R. Rosa, "Filler toughening of plastics. Part 1—the effect of surface interactions on physico-mechanical properties and rheological behaviour of ultrafine CaCO<sub>3</sub>/HDPE nanocomposites," *Polymer*, vol. 46, no. 3, pp. 827–844, 2005.
- [12] Z. Bartzczak, A. S. Argon, R. E. Cohen, and M. Weinberg, "Toughness mechanism in semi-crystalline polymer blends: II. High-density polyethylene toughened with calcium carbonate filler particles," *Polymer*, vol. 40, no. 9, pp. 2347–2365, 1999.
- [13] Y. Lin, H. Chen, C.-M. Chan, and J. Wu, "High impact toughness polypropylene/CaCO<sub>3</sub> nanocomposites and the toughening mechanism," *Macromolecules*, vol. 41, no. 23, pp. 9204–9213, 2008.
- [14] Y. S. Thio, A. S. Argon, R. E. Cohen, and M. Weinberg, "Toughening of isotactic polypropylene with CaCO<sub>3</sub> particles," *Polymer*, vol. 43, no. 13, pp. 3661–3674, 2002.
- [15] P. Yuan, P. D. Southon, Z. Liu et al., "Functionalization of halloysite clay nanotubes by grafting with  $\gamma$ -aminopropyltriethoxysilane," *The Journal of Physical Chemistry C*, vol. 112, no. 40, pp. 15742–15751, 2008.
- [16] E. Joussein, S. Petit, J. Churchman, B. Theng, D. Righi, and B. Delvaux, "Halloysite clay minerals—a review," *Clay Minerals*, vol. 40, no. 4, pp. 383–426, 2005.
- [17] Z. Xu, Y. Niu, L. Yang et al., "Morphology, rheology and crystallization behavior of polylactide composites prepared through addition of five-armed star polylactide grafted multiwalled carbon nanotubes," *Polymer*, vol. 51, no. 3, pp. 730–737, 2010.
- [18] K. Madhavan Nampoothiri, N. R. Nair, and R. P. John, "An overview of the recent developments in polylactide (PLA) research," *Bioresource Technology*, vol. 101, no. 22, pp. 8493–8501, 2010.
- [19] A. M. Harris and E. C. Lee, "Improving mechanical performance of injection molded PLA by controlling crystallinity," *Journal of Applied Polymer Science*, vol. 107, no. 4, pp. 2246–2255, 2008.
- [20] K. S. Anderson and M. A. Hillmyer, "Melt preparation and nucleation efficiency of polylactide stereocomplex crystallites," *Polymer*, vol. 47, no. 6, pp. 2030–2035, 2006.
- [21] S. C. Schmidt and M. A. Hillmyer, "Polylactide stereocomplex crystallites as nucleating agents for isotactic polylactide," *Journal of Polymer Science B: Polymer Physics*, vol. 39, no. 3, pp. 300–313, 2001.
- [22] H. Tsuji, H. Takai, and S. K. Saha, "Isothermal and non-isothermal crystallization behavior of poly(l-lactic acid): effects of stereocomplex as nucleating agent," *Polymer*, vol. 47, no. 11, pp. 3826–3837, 2006.
- [23] Y. Lin, H. B. Chen, C.-M. Chan, and J. S. Wu, "Nucleating effect of calcium stearate coated CaCO<sub>3</sub> nanoparticles on polypropylene," *Journal of Colloid and Interface Science*, vol. 354, no. 2, pp. 570–576, 2011.
- [24] C.-M. Chan, J. S. Wu, J.-X. Li, and Y.-K. Cheung, "Polypropylene/calcium carbonate nanocomposites," *Polymer*, vol. 43, no. 10, pp. 2981–2992, 2002.
- [25] M. Liu, B. Guo, M. Du, F. Chen, and D. Jia, "Halloysite nanotubes as a novel  $\beta$ -nucleating agent for isotactic polypropylene," *Polymer*, vol. 50, no. 13, pp. 3022–3030, 2009.
- [26] S.-H. Lee, S. Wang, and Y. Teramoto, "Isothermal crystallization behavior of hybrid biocomposite consisting of regenerated cellulose fiber, clay, and poly(lactic acid)," *Journal of Applied Polymer Science*, vol. 108, no. 2, pp. 870–875, 2008.
- [27] H. Li and M. A. Huneault, "Effect of nucleation and plasticization on the crystallization of poly(lactic acid)," *Polymer*, vol. 48, no. 23, pp. 6855–6866, 2007.
- [28] E. W. Fischer, H. J. Sterzel, and G. Wegner, "Investigation of the structure of solution grown crystals of lactide copolymers by means of chemical reactions," *Colloid and Polymer Science*, vol. 251, no. 11, pp. 980–990, 1973.
- [29] A. J. Nijenhuis, E. Colstee, D. W. Grijpma, and A. J. Pennings, "High molecular weight poly(L-lactide) and poly(ethylene oxide) blends: thermal characterization and physical properties," *Polymer*, vol. 37, no. 26, pp. 5849–5857, 1996.
- [30] Y. S. Thio, A. S. Argon, and R. E. Cohen, "Role of interfacial adhesion strength on toughening polypropylene with rigid particles," *Polymer*, vol. 45, no. 10, pp. 3139–3147, 2004.
- [31] G. Z. Papageorgiou, D. S. Achiliadis, S. Nanaki, T. Beslikas, and D. Bikiaris, "PLA nanocomposites: effect of filler type on non-isothermal crystallization," *Thermochimica Acta*, vol. 511, no. 1–2, pp. 129–139, 2010.

- [32] L. Petersson and K. Oksman, "Biopolymer based nanocomposites: comparing layered silicates and microcrystalline cellulose as nanoreinforcement," *Composites Science and Technology*, vol. 66, no. 13, pp. 2187–2196, 2006.
- [33] Z. Kulinski and E. Piorkowska, "Crystallization, structure and properties of plasticized poly(L-lactide)," *Polymer*, vol. 46, no. 23, pp. 10290–10300, 2005.
- [34] M. Pluta, "Morphology and properties of polylactide modified by thermal treatment, filling with layered silicates and plasticization," *Polymer*, vol. 45, no. 24, pp. 8239–8251, 2004.
- [35] M. Murariu, A. D. S. Ferreira, M. Pluta, L. Bonnaud, M. Alexandre, and P. Dubois, "Polylactide (PLA)-CaSO<sub>4</sub> composites toughened with low molecular weight and polymeric ester-like plasticizers and related performances," *European Polymer Journal*, vol. 44, no. 11, pp. 3842–3852, 2008.
- [36] K. Molnar, J. Moczó, M. Murariu, P. Dubois, and B. Pukanszky, "Factors affecting the properties of PLA/CaSO<sub>4</sub> composites: homogeneity and interactions," *eXPRESS Polymer Letter*, vol. 3, pp. 49–61, 2009.
- [37] X. T. Shi, R. Rosa, and A. Lazzeri, "On the coating of precipitated calcium carbonate with stearic acid in aqueous medium," *Langmuir*, vol. 26, no. 11, pp. 8474–8482, 2010.
- [38] G.-M. Kim and G. H. Michler, "Micromechanical deformation processes in toughened and particle-filled semicrystalline polymers: part 1. Characterization of deformation processes in dependence on phase morphology," *Polymer*, vol. 39, no. 23, pp. 5689–5679, 1998.
- [39] G.-M. Kim and G. H. Michler, "Micromechanical deformation processes in toughened and particle filled semicrystalline polymers. Part 2. Model representation for micromechanical deformation processes," *Polymer*, vol. 39, no. 23, pp. 5699–5703, 1998.



# Hindawi

Submit your manuscripts at  
<http://www.hindawi.com>

